



EXPERIMENTATION AND ANALYSIS OF THE HEAT TRANSFER BEHAVIOUR OF THE HYBRID NANOFLUID ($\text{Al}_2\text{O}_3 + \text{ZnO}$) IN A PARALLEL FLOW HEAT EXCHANGER

Veerababu Divili¹

¹Department of Mechanical Engineering, UCEK(A)
JNTUK 533003, Andhra Pradesh, India.

ABSTRACT

Estimating the heat transfer enhancement for various Reynolds numbers in turbulent ranges at a volume concentration of 0.1% is the goal of the current investigation. Compared to conventional heat transfer fluids, nanofluids are thought to be new-generation fluids with superior heat transfer properties. There is a lot of promise for heat transfer applications with the nanofluid, a new field of study. Thermophysical characteristics of ZnO and Al_2O_3 at varying volume concentrations have been experimentally evaluated using a mixture of water & Mono Ethylene Glycol as the basis fluid. The thermo-physical properties of the combination are greatly enhanced when metal oxide hybrid nanoparticles are suspended in the base fluid. The outcomes of studies on a hybridized nanofluid mixture ($\text{Al}_2\text{O}_3.\text{ZnO}$) show exceptional thermophysical characteristics. As a result, we can specify a 60:40 $\text{Al}_2\text{O}_3.\text{ZnO}$ mixture that yields promising outcomes in both an economical and experimental manner. $\text{Al}_2\text{O}_3.\text{ZnO}$ will have numerous opportunities to improve their performance through small-scale industrial applications. Compact heat exchanger design and high-energy device miniaturization are only feasible with fluids that perform better in heat transfer.

Keywords: Nanomaterials, Compact Heat exchanger, Reynolds Number, Hybridization, Heat transfer Enhancement.

Cite this Article: Veerababu Divili. Experimentation and Analysis of the Heat Transfer Behaviour of the Hybrid Nanofluid ($Al_2O_3 + ZnO$) in a Parallel Flow Heat Exchanger. *International Journal of Thermal Engineering (IJTE)*, 13(1), 2025, pp. 1-38.

https://iaeme.com/MasterAdmin/Journal_uploads/IJTE/VOLUME_13_ISSUE_1/IJTE_13_01_001.pdf

1. Introduction

The primary objective of this research is the application of nanofluids in heat exchangers. The capacity expansion of many industries is hampered by the incapacity of heat devices to react to higher capacities. Furthermore, one of the most significant constraints for major enterprises is the pressure drop, which results from growing capacity. The use of special nanofluids can greatly increase the thermal efficiency of the heat exchanger, one of the most crucial thermal devices in the industry, while conventional methods of increasing heat transfer significantly increase the pressure drop. This includes an introduction to nanofluids, followed by an examination of how experiments have been used to determine how nanofluids affect heat exchanger efficiency. In addition to being crucial for energy conversion, improving the thermal and hydraulic performance of heat exchangers also helps systems recover economically through savings.

NANOFLUIDS:

A fluid that contains nanoparticles—metal particles that are nanometers in size—is referred to as a nano fluid. These nanofluids are created using a number of techniques to create a colloidal suspension of nanoparticles in a base fluid. Nanoparticles are used in nano fluids and are often made of metals, oxides, carbides, or carbon nanotubes. Al_2O_3 , CuO , TiO_2 , CeO_2 , and SiO_2 are examples of common nanoparticles. Water, ethylene glycol, and oil are examples of base fluids. The two main prerequisites for studying nanofluids are their synthesis and stability. [1]

The appealing characteristics of nanoparticles—a huge surface area, low particle momentum, and fast mobility—made them suitable candidates for suspension in fluids. Multi-walled carbon nanotubes (MWCNTs), which at normal temperature have 20,000 times the conductivity of motor oil, are the next step up from copper in terms of conductivity increase [2].

Particle size is the primary determinant because as particle size reduces, a molecule's area of contact rises and its void spaces also reduce, making nanoparticles effective heat conductors.

However, thermal conductivity, viscosity, and a few other specifics continue to be the focus of most contemporary study. Since thermal conductivity depends on material viscosity and specific heat, it is evident that an increase in viscosity could counteract an increase in thermal conductivity and result in a fall in effective specific heat. Properly constructed thermal nanofluids provide the following benefits over traditional solid-liquid suspensions for heat transfer intensification [3]:

- More heat transfer surface between particles and fluids due to a high specific surface area.
- Outstanding dispersion stability and a high degree of Brownian motion.
- To get the same heat transfer, less pumping force is needed than with a pure liquid.
- Less particle clogging than with traditional slurries, which encourages system downsizing.

The thermal characteristics of carbon nanotubes were emphasized in early studies by Kim et al. (2001) [2], while Wen et al. (2009) [3] pointed out drawbacks in nanofluid formulations. Research by Wen & Ding (2006) [6] and Lee & Mudawar (2005) [5] showed improved heat transmission in both macro and micro channels, especially in laminar flows. Nield & Kuznetsov (2009) [9] pointed out that thermophoresis and Brownian motion can lower the Nusselt number, while Chein & Chuang (2007) [7] reported better heat dissipation with CuO nanofluids.

For improved heat transmission, Koo & Kleinstreuer's (2008) numerical studies [10,11] suggested base fluids with a high Prandtl number and ideal nanoparticle volume fractions (~4%). According to Louis et al. (2016) [16], metallic oxides (MgO, TiO_2 , and ZnO) can improve heat transmission by as much as 30%. According to Hussein et al. (2018) [19], SiO_2 nanofluids increased heat transmission in automobile radiators by 50%. Bahmani et al. (2019, 2021) [29,30] showed that increased Reynolds numbers greatly increase heat transfer efficiency in heat exchangers. According to Poongavanam et al. (2020) [31] and Zhen et al. (2021) [32], heat transport was enhanced by 44.3% and 32.5%, respectively, using CuO and SiO_2 nanofluids. According to Routbort et al. (2008) [33], the industrial use of nanofluids could result in yearly savings of 10–30 trillion Btu. According to Wole-Osho et al. (2020) [41], hybrid Al_2O_3 -ZnO nanofluids reduced specific heat by 30.12% and enhanced viscosity by 96.37%. In this

experimenting work, developing a hybrid Al₂O₃/ZnO nanofluid at different ratio of mixtures to increase the rate of heat transfer at different concentrations in heat exchangers and Obtain Optimum ratio. The creation of nanoparticles for heat transfer applications by employing a particular preparation technique and stabilizing the nano-fluid with additives.

Heat exchangers are utilized across various industries. They are essential in thermal power plants (e.g., boilers, superheaters, steam condensers), refrigeration and air conditioning systems (e.g., evaporators, condensers, coolers), and automobile industries (e.g., radiators and engine cooling systems). The chemical process industry relies on heat exchangers for fluid heat exchange in combustors and reactors, while the cryogenic industry employs them in distillation columns and gas production from cryogenic liquids. Additionally, research applications include ceramic heat exchangers for ultra-low-temperature devices and superconducting magnet systems. Heat exchangers are essential for effective energy transfer and are always changing to satisfy industrial needs.

Main Factors Affecting Heat Transfer Rate in Heat exchangers: The heat transfer rate in nanofluids is influenced by multiple factors, including viscosity, density, nanoparticle concentration, and flow regime.

a. Effects of Viscosity on Heat Transfer and Pressure Drop:

Viscosity (μ) is a critical parameter affecting pressure drop (ΔP) and pumping power. It is inversely proportional to temperature and is influenced by nanoparticle size, shape, and volume concentration. The viscosity of nanofluids can be expressed as:

$$\mu_{nf} = \mu_{bf}(1 + 2.5\phi)$$

where μ_{nf} is the nanofluid viscosity, μ_{bf} is the base fluid viscosity, and ϕ is the volume concentration of nanoparticles. Increased viscosity leads to a higher pressure drop, as shown by:

$$\Delta P \propto \mu$$

b. Effects of Density on Heat Transfer Rate:

Density (ρ) plays a significant role in Reynolds number (Re), friction factor, and pressure drop. Nanofluid density is inversely proportional to temperature and depends on nanoparticle properties and base fluid density. It is calculated as:

$$\rho_{nf} = \phi\rho_p + (1-\phi) * \rho_{bf}$$

where ρ_{nf} is the nanofluid density, $\phi\rho_p$ is the particle density, and ρ_{bf} is the base fluid density. The Reynolds number, which determines the flow regime, is given by:

$$Re = \rho V D / \mu$$

where V is velocity and D is the characteristic length.

c. Effects of Nanoparticle Concentration on Heat Transfer:

Nanoparticle concentration (ϕ) directly affects the heat transfer coefficient (h) and Nusselt number (Nu). Increasing concentration improves heat transfer but also increases pressure drop and pumping power requirements. The heat transfer coefficient is given by:

$$h = k / dt$$

where k is thermal conductivity and dt is the thermal boundary layer thickness. The Nusselt number (Nu), which measures convective heat transfer enhancement, is influenced by nanoparticle migration and flow characteristics:

$$Nu \propto Re^{0.8} Pr^{0.33}$$

where Pr is the Prandtl number. The presence of nanoparticles also alters boundary layer development, leading to increased thermal efficiency in turbulent flows. The combination of higher viscosity, density, and nanoparticle concentration leads to heat transfer enhancement, but excessive viscosity and pressure drop can negatively impact system performance. Optimizing nanoparticle concentration, base fluid properties, and flow conditions is essential for maximizing efficiency in heat exchanger applications

Properties of Nanofluids

Thermal conductivity, viscosity, density, specific heat, and surface tension are considered some main thermo physical properties of nanofluids. Various parameters like nano

particle type, size, and shape, volume concentration, fluid temperature, and nanofluid preparation method influence the thermophysical properties of nanofluids [2].

- Viscosity of fluid
- Density of nanofluids
- Thermal Conductivity of fluid

Merits and Demerits of nanofluids in heat exchangers

Merits:

Pressure drop increases with increasing nanoparticle concentration when compared to pure fluids at the same Reynolds number. Compared to the base fluid alone, nanoparticles increase the rate of heat transfer. Because of their high aspect ratio and conductivity, nanoparticles are perfect for usage in microchannels that can handle significant heat inputs. By using them, the risk of clogging that comes with bigger particles is avoided. Heat transport is facilitated by micro convection, which is made possible by the molecules' small size.

DEMERITS:

Increased pumping power because of longer-term fluid settling and increased pressure drop, which may clog flow channels and cause erosion-related damage to flow loop components. Inability to maintain boiling of the flow. Suspension of nanoparticles is expensive.

2. Materials

The project started with the acquisition of 500 grams of alumina oxide (Al_2O_3) that met the necessary purity and mesh size requirements. For heat transfer applications, 8 liters of mono-ethylene glycol (MEG) are recommended because of its superior thermal characteristics, low viscosity, and total water miscibility. It was utilized in research and kept in plastic containers. 35 liters of De-Ionized Water (DW) are also needed, with a neutral pH of 7 to facilitate mixing with MEG. Zinc chloride ($ZnCl_2$), sodium hydroxide (NaOH), and acetic acid were needed for the manufacture of zinc oxide (ZnO) nanoparticles using the new sol-gel technique.

Experimentation and Analysis of the Heat Transfer Behaviour of the Hybrid Nanofluid ($Al_2O_3 + ZnO$) in a Parallel Flow Heat Exchanger

Table (1): Specifications of obtained Al_2O_3

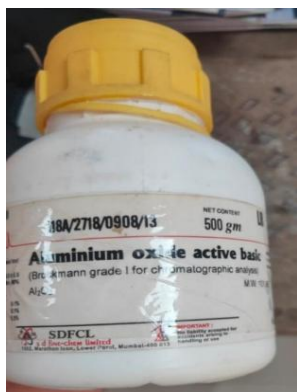


FIG (1): 500gms of Al_2O_3

| | |
|----------------------------|------------------|
| Suitability Test | Passes |
| P (10% aqueous suspension) | 9.5 ± 0.5 |
| Mesh Size | 100-300(0.074mm) |
| Limits of impurities: C1 | 0.1% |
| Sulphate (SO_4) | 0.1% |
| Water Solubles | 0.1% |

Table (2): Properties of mono ethylene glycol



FIG (2): 8ltr of MEG

| | |
|-----------------------|------------------|
| Molecular weight | 62.07g/mol |
| Auto ignition temp | $396^{\circ}C$ |
| Dynamic viscosity | 19.83 mPa-s |
| Normal freezing point | $-11.2^{\circ}C$ |
| Normal boiling point | $195^{\circ}C$ |
| Specific gravity | 1.1153 |
| Vapor density | $2.1Kg/m^3$ |
| Solubility in water | 100wt% |

Table (3): Properties of de-ionized water



Fig (3): De-ionized water

| | |
|---------------------|----------------------------------|
| Density | $998 kg/m^3$ |
| Viscosity | $1.00 \times 10^{-3} Pa-s$ |
| Kinematic Viscosity | $1.00 \times 10^{-6} m^2/s$ |
| Surface tension | $7.28 \times 10^{-2} N/m$ |
| Bulk modulus | 2.12 Gpa |
| Thermal Expansion | $2.07 \times 10^{-4} /^{\circ}C$ |



Fig (4): Sodium Hydroxide pellets, Zinc Chloride

Modification in Heat Exchanger:

The former heat exchanger was a shell and tube double pipe heat exchanger with the following dimensions:

Inner tube: Inner diameter- 8.5mm

Outer tube: Inner diameter- 27.5mm

Outer diameter- 14.0mm

Outer diameter- 33.5mm

Length of the heat exchange division: 2m



Fig (5): Former shell and tube double pipe heat exchanger

It is made for the measurement of heat transfer characteristics such as

(a) Heat Transfer, Q

(b) Logarithmic Mean Temperature Difference, LMTD

(c) Effectiveness (ϵ)

(d) Overall Heat Transfer Coefficient, OHTC, only for water as cold fluid and hot fluid as well.

Since the replacement for the cold fluid will be the coolant produced, certain changes in the passage of the heat exchanger were made:

- **Stand:** To achieve the desired flow rate for the coolant as cold fluid, a small stand was designed and installed at a height of 3 meters using a semi-circular wooden base to hold the coolant tank and two L clamps drilled on the wall to support this wooden platform.
- **Cold Side modification:** A T joint was enabled at the beginning of the cold-water inlet tap through which either water or the coolant can flow. While working with the different samples of coolant as cold fluid, the normal tap water is closed with the help of a valve. The valve on the coolant side was made open for experimentation. This passage from the T joint was connected to a 1.5m hose pipe whose other end was attached to the tank installed at the top as shown in the figure below.
- **Hot side modification:** Initially, tap water was used to serve as the source for hot and cold water. One water passage was diverted which would go inside the heater of the

heat exchanger and come out with raised temperature as the hot fluid inlet. Since the tap water source is switched off through the primary valve hence, another hose pipe of 5 meters was attached to the heater inlet through an external tap providing water. Thereby, hot fluid was set as water and cold fluids were different coolant samples.



Fig (6): Modified heat exchanger

3. Preparation of Nanofluid

Preparation of Aluminium Oxide:

Ball milling was used to reduce aluminium oxide particle size. A 1:3 powder-to-ball ratio was maintained using 30.1 g of Al_2O_3 and 90.3 g of tungsten carbide. Tungsten balls and the wale were thoroughly cleaned, first with scrubber and then with ethanol to avoid any previous residue left. The process was conducted in a planetary mill at 200 RPM for 4.5 hours with intermittent cooling for 10 minutes of halt had been taken to avoid overheating of the motor after every 1 hr. to prevent overheating. The obtained Al_2O_3 nano powder was carefully collected and stored.

Zinc Oxide (ZnO) Preparation via Sol-Gel Method:

Aqueous Zinc Chloride (ZnCl_2) solution (0.2M, 50 ml) was prepared using 1.3628 g ZnCl_2 , and NaOH solution (8M, 50 ml) was prepared with 16 g NaOH. The NaOH solution was

added dropwise into the $ZnCl_2$ solution at 600 RPM until pH 7 was achieved, forming a curd-like ZnO precipitate.

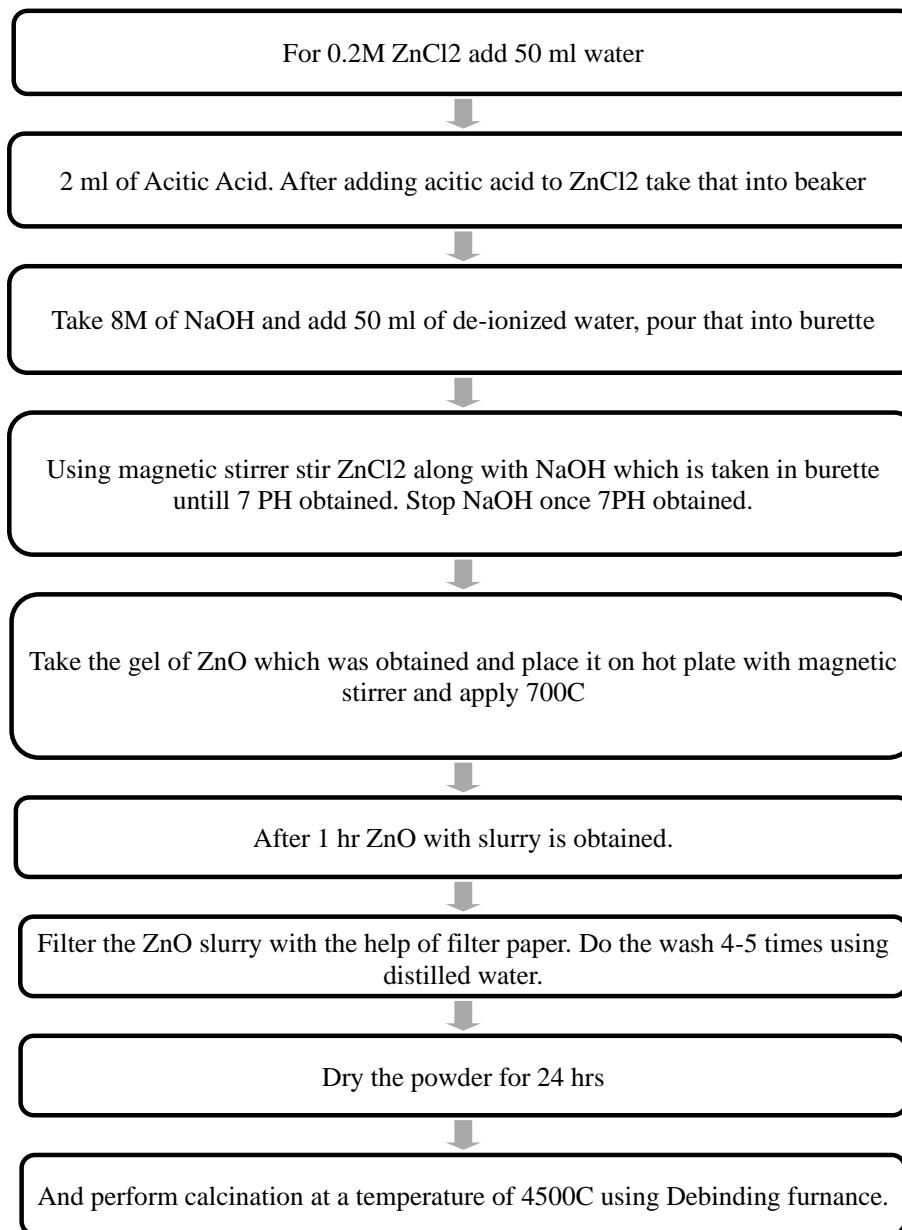


One 22-foot pieces of filter paper were ripped in half, and each half was folded into a funnel shape. As seen in the figure, both funnels are placed on the round-bottom filter flask after being overlapped to create a single funnel. The hot zinc chloride was gently put into the funnel to cool. De-ionized water was put into the funnel to filter the solution as much as possible, even though the water content had totally decreased into the filter flask after a few hours. The solution was filtered, dried for 24 hours, and collected in batches of 3 g per iteration, completing 14 iterations to obtain 42 g of ZnO nanoparticles.

Calcination Of Zinc Oxide:

Zinc Oxide (ZnO) calcination is the process of heating a chemical to a certain temperature to eliminate any impurities, volatile substances, or salts. The temperature range for calcination in a muffle furnace is 400–12,000C. A De-binding machine with a temperature range of 300-7000C was used to calcine zinc oxide (ZnO), which requires a temperature of 4500C. The furnace contains two crucibles that can hold 15 grams of ZnO each. After thorough cleaning, distilled water was used to rinse these crucibles. A screw mechanism opened the furnace's lid, and a dry towel was used to wipe away any dust inside. Each crucible was filled with ZnO powder, carefully placed into the furnace, and had its outer cap secured. Crucibles must be positioned carefully to prevent powder from falling into the chamber because it is a vertical cylindrical space with a diameter of 15 cm. The machine's temperature was set to 4500C. After two hours of soaking, the furnace is turned off and the calcination is carried out for two more hours. After the cooling period the ZnO powder is stored in an airtight container to avoid oxidization.

Flow chart for the preparation:



Hybridization:

Hybridization is the process of combining two distinct component types in a particular ratio while maintaining each type's unique characteristics. ZnO and Al₂O₃ have exceptional thermophysical characteristics. Five liters of nano-coolant total—three liters of de-ionized water and two liters of nano-ethylene glycol—had to be manufactured for a single coolant sample. Additionally, three samples with the following ratios of Al₂O₃ to ZnO were to be produced: 80:20, 50:50, and 60:40 [Al₂O₃: ZnO], respectively. The exact weight of the nanoparticles was determined by mixing 0.1% of these metal oxides by volume in the base fluid.

5 ml is equal to 0.1vol% for 5 liters.

Case 1: For 80:20 [Al_2O_3 : ZnO] sample, 4 ml of Al_2O_3 and 1ml of ZnO must be converted into mass using the formula, [Density = mass/volume]. Thereby obtaining 15.520gms of Al_2O_3 and 5.600 gm of ZnO as weight of each metal oxide nano particle, which were to be hybridized in the planetary mill and then mixed through sonification in the base fluid.

Case 2: For 60:40 [Al_2O_3 : ZnO] sample, 3ml of Al_2O_3 and 2 ml of ZnO must be converted into mass using the same density- mass relationship formula and the following weights were obtained, Al_2O_3 : 12.640 gm and ZnO: 11.200 gm.

Case 3: For 50:50 [Al_2O_3 : ZnO] sample, 2.5 ml of each must be converted into mass using density-mass relationship formula and the following weights were obtained, Al_2O_3 : 9.7 gm and ZnO: 14 gm.

With an error of ± 0.1 grams, the weights were precisely measured in a precision balance. After four and a half hours of ball milling with a 1:5 powder to ball ratio, the three samples were abraded from the wale and balls and gathered.

Sonification of metal oxides in base fluid:

Sonification of metal oxides in base fluid: Using a probe sonicator to sonicate a solution effectively disperses nanoparticles. The mixture is stirred, and the nanoparticles are uniformly dissolved in the solution by the sonicator's ultrasonic. Monoethylene glycol with de-ionized water required to be used as the basis fluid for sonicating the three hybrid metal oxide mixtures. The process of ultrasonication was used.

The following nano-coolants/samples were prepared through probe sonicator:

1. 3 liters of de-ionized water + 2 liters of Mono-ethylene glycol.
2. 3 liters of DW + 2 liters of MEG + 80:20[Al_2O_3 : ZnO].
3. 3 liters of DW + 2 liters of MEG + 60:40[Al_2O_3 : ZnO].
4. 3 liters of DW + 2 liters of MEG + 50:50[Al_2O_3 : ZnO].

Three liters of DW and two liters of MEG were weighed using a measuring jar and then transferred into a sanitized container. The solution was obtained in 5 liters. It seemed as transparent as water (DW + MEG). The platform where the container was to be stored had a wooden base. The container was carefully stored to prevent any falls. As the probe was submerged in the coolant, two levers that were supposed to be part of the probe were loosened until the container was properly positioned. The equipment timer was set for 30 minutes after the main switch was turned on. At 210V the machine was switched on as high frequency can

be heard while the probe sonicator starts working. Four time-intervals were used during the two-hour sonication process. The primary switch was shut off as soon as the high frequency ceased. The probe was drawn up and tightened when both levers were loosened. The sample container was carefully removed and transferred to a 5-liter can that had been completely cleaned and rinsed.

Sonication was carried out for three different nano-coolant samples with varying Al₂O₃:ZnO ratios. For the 80:20 sample (21.12 g of hybrid mixture), the powder was finely crushed before being mixed with 3 liters of de-ionized water (DW) and 2 liters of mono-ethylene glycol (MEG). The solution turned ash-colored as the metal oxides dissolved, and it was initially stirred with a glass rod before being placed on the sonication platform. The 60:40 sample was similarly added to the 5-liter base fluid, and sonication was performed for 2 hours at 210V and a constant frequency rate. The processed sample was then collected in a cleaned container. For the 50:50 sample, the same sonication procedure was followed, ensuring uniform dispersion of nanoparticles in the fluid. Each sample was carefully handled and stored after sonication.

4. Properties of Nanofluid

Density of coolant samples:

Due to the unavailability of a density meter, values of density were calculated mathematically using the formula and a precision balance weighing machine with ± 0.1 gm error. Using the standard formula

$$\rho = \frac{m_a}{V_a} + \frac{m_b}{V_b}$$

Table (4): Sample name and their densities.

| Sample name | Density(kg/m ³) |
|-------------|-----------------------------|
| DW+MEG | 1059.68 |
| 80:20:00 | 1059.817 |
| 50:50:00 | 1062.96 |
| 60:40:00 | 1062.23 |

Viscosity testing:

The viscosity of four nano-coolant samples was tested using a Redwood Viscometer. The test aimed to determine both kinematic and absolute viscosity. The required apparatus included two thermometers, a stopwatch, and a 50 ml flat-bottomed flask. The experiment began with cleaning and drying the flask, leveling the apparatus, and filling the heating bath with water above the hook gauge level.

Sample 1 (DW + MEG) was poured into the oil cup, and a 50 ml flask was positioned below the orifice. The initial temperature of the pure water in the oil cup was recorded before opening the orifice to measure the time taken for 50 ml to flow into the flask. The heating bath temperature was then increased by 5°C, followed by stirring to reach thermal equilibrium. This process was repeated for six iterations to observe changes in viscosity. As the temperature increased, the viscosity decreased, leading to a reduction in the time taken for the coolant to fill the flask. However, the variations in viscosity were minimal compared to conventional oils, indicating that the nano-coolant maintained relatively stable viscosity characteristics.

Recorded viscosity readings for all samples:

a. DW+MEG

Table (5): Viscosity values of DW+MEG Sample by temperature against time

| S. No | Temperature (T ⁰ C) | Time taken for 50 ml (sec) |
|-------|--------------------------------|----------------------------|
| 1 | 30 | 33 |
| 2 | 35 | 31 |
| 3 | 40 | 30 |
| 4 | 45 | 28 |
| 5 | 50 | 27 |
| 6 | 57 | 27 |

b. 80:20 [Al₂O₃: ZnO] + DW+MEG**Table (6):** Viscosity values of 80:20 Sample by temperature against

| S. No | Temperature (T ⁰ C) | Time taken for 50 ml (sec) |
|-------|--------------------------------|----------------------------|
| 1 | 32 | 56.29 |
| 2 | 43 | 49.38 |
| 3 | 51 | 39.56 |
| 4 | 59 | 28.41 |
| 5 | 65 | 27.46 |
| 6 | 69 | 27.08 |

c. 50:50 [Al₂O₃: ZnO] + DW+MEG**Table (7):** Viscosity values of 50:50 Sample by temperature against time

| S. No | Temperature (T ⁰ C) | Time taken for 50 ml (sec) |
|-------|--------------------------------|----------------------------|
| 1 | 32 | 53.34 |
| 2 | 43 | 46.29 |
| 3 | 51 | 41.35 |
| 4 | 59 | 27.56 |
| 5 | 65 | 27.28 |
| 6 | 69 | 27.11 |

d. 60:40 [Al₂O₃: ZnO] + DW+MEG**Table (8):** Viscosity values of 60:40 Sample by temperature against time

| S. No | Temperature (T ⁰ C) | Time taken for 50 ml (sec) |
|-------|--------------------------------|----------------------------|
| 1 | 32 | 54.31 |
| 2 | 43 | 49.46 |
| 3 | 51 | 44.43 |
| 4 | 59 | 28.68 |
| 5 | 65 | 27.41 |
| 6 | 69 | 27.26 |

Experimentation and Analysis of the Heat Transfer Behaviour of the Hybrid Nanofluid (AL₂O₃ + ZnO) in a Parallel Flow Heat Exchanger

Kinematic viscosity of the coolant samples was determined by using the equation

$$K.V = At-B/t$$

Where, A = 0.26 centistokes, when the time taken to fill 50 ml is more than 20 sec

B = 172 centistokes, when the time to fill 50 ml is less than 20 sec.

t = time taken to fill 50 ml at certain temperature.

Dynamic viscosities were obtained by the product of kinematic viscosity and density of coolant sample.

$$D.V=KV \times \rho$$

Where, DV = Dynamic viscosity [centipoise]

KV = Kinematic viscosity [centistokes]

ρ = density of the coolant sample [gm/cc]

Table (9): The respective values of viscosities for all the coolant samples.

| S. No | Sample Name | Density (gm/cc) | Kinematic Viscosity (centistokes) | Dynamic Viscosity (centipoise) |
|-------|-------------|-----------------|-----------------------------------|--------------------------------|
| 1 | DW + MEG | 1.05968 | 2.795 | 2.96 |
| 2 | 40:60 | 1.06223 | 10.9535 | 11.63513 |
| 3 | 50:50:00 | 1.06296 | 10.6438031 | 11.31393 |
| 4 | 80:20:00 | 1.059817 | 11.57979 | 12.2724583 |

Crystallite size determination:

XRD Analysis of 4 samples had been tested. It is used to determine the size of the crystal in the composition. X-ray diffraction can be used to determine the size of a crystal (crystallite size) with a phase certain. The determination refers to the main peaks of the pattern diffractogram through the approach Debye Scherrer's equation formulated in Equation

$$D= K*\lambda /\beta \cos \theta$$

where, D is the crystallite size,

K is the Scherrer constant (0.9)

λ is the wavelength of the X-rays used (0.15406 nm)

β is the Full Width at Half Maximum (FWHM, radians)

θ is the peak position (radians).

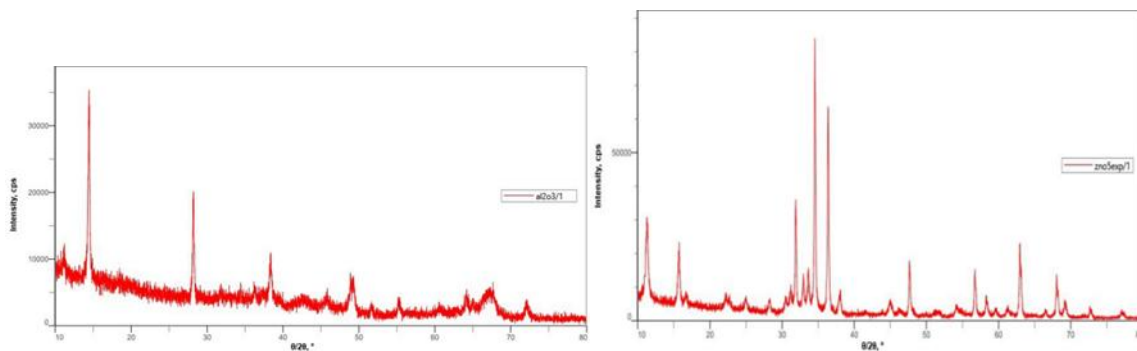


Fig (7): Intensity curves of Al_2O_3 and ZnO

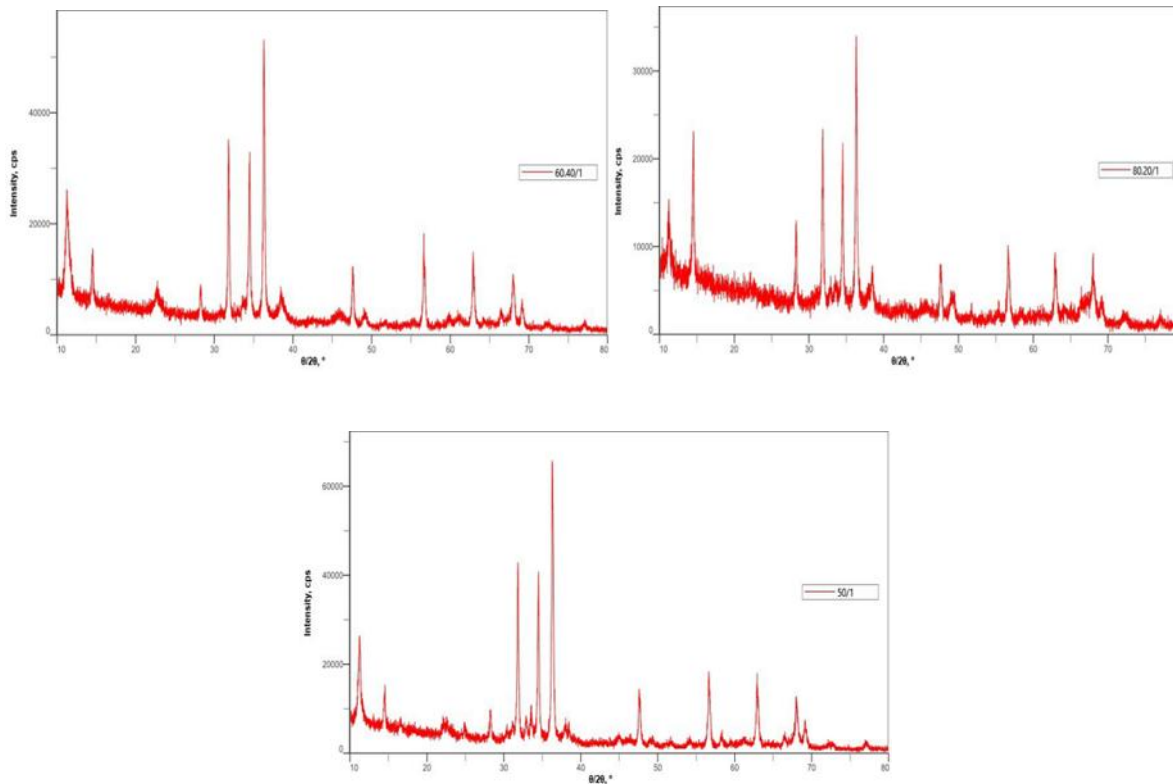


Fig (8): Intensity curves of three samples

Based on curves obtaining the required data and determined the crystallite size obtained.

Table (10): Crystallite size based on the XRD data

| S. No | Sample Name | β (radians) | 2 θ | D(crystallite size) |
|-------|--------------------------------|-------------------|------------|---------------------|
| 1 | Al ₂ O ₃ | 0.0032 | 14.44 | 47.69 |
| 2 | ZnO | 0.0034 | 34.54 | 40.63 |
| 3 | 60:40:00 | 0.0033 | 36.29 | 40.96 |
| 4 | 50:50:00 | 0.0032 | 36.29 | 41.03 |
| 5 | 80:20:00 | 0.0035 | 36.28 | 41.02 |

5. Experimentation

To determine the heat transfer performance of the coolant samples, testing was carried out on double pipe shell & tube heat exchanger

Case 1: [DW+MEG]: De-ionized water and mono ethylene glycol coolant sample of 5 liters must be tested first. The coolant storage can was well shaken first before pouring into the reservoir. All the valves were closed till the coolant sample filled in the stand tank. Parallel flow arrangement had to be kept initially. Now the water source for hot fluid was open and its flow rate had been calculated using measuring jars and stopwatch at 1.5 ltr/min & coolant sample was set at 3 ltr/min. Both the fluids start flowing uniformly which can be observed at the outlets of the heat exchangers. Firstly, the temperatures were note down after 10 minutes and later on the temperatures has to be measured after 5 minutes. Temperature values are noted down from the thermometer as follows:

T_{hi}- Temperature at hot water inlet

T_{ho} – Temperature at hot water outlet

T_{ci} – Temperature at cold water inlet

T_{co} – Temperature at cold water outlet

Time was checked after every 5 min and readings were noted down. The thermometer readings of hot and cold-water inlet & outlet temperatures were noted down. This process was repeated until steady state condition is attained. The table below gives the output from the first test.

After successfully reached the steady state condition, the heater was switched off and the heat exchanger was turned off. Now the test was carried for a different flow rate, i.e., 600 ml/min a hot water and 1400 ml/min a cold water flow rates. The flow rates have been set, and

the valves were arranged in parallel flow position and the same procedure was followed and the respective readings are noted down.

The following table shows the temperatures at the different flow rate.

Table (11): Temperatures at 1.5 lt/min hot water flow rate data

| S. No | Time | Hot water side | | | Water +Ethylene Glycol | | |
|-------|------|-------------------|-----------------------------|------------------------------|------------------------|-----------------------------|-------------------------------|
| | | Flow Rate(lt/min) | Inlet temp(⁰ C) | Outlet temp(⁰ C) | Flow rate(lt/min) | Inlet temp(⁰ C) | Outlet temp (⁰ C) |
| 1 | 0 | 1.5 | 28 | 28 | 3 | 28 | 28 |
| 2 | 10 | 1.5 | 53 | 47 | 3 | 33 | 35 |
| 3 | 15 | 1.5 | 52.5 | 47 | 3 | 35.5 | 37 |
| 4 | 20 | 1.5 | 52 | 48 | 3 | 37.5 | 38.5 |
| 5 | 25 | 1.5 | 52.5 | 48.5 | 3 | 38.5 | 39.5 |
| 6 | 30 | 1.5 | 52.5 | 48.5 | 3 | 38.5 | 39.5 |

Table (12): Temperatures at 0.6 lt/min hot water flow rate data

| S. No | Time | Hot water side | | | Water +Ethylene Glycol | | |
|-------|------|-------------------|-----------------------------|------------------------------|------------------------|-----------------------------|-------------------------------|
| | | Flow Rate(lt/min) | Inlet temp(⁰ C) | Outlet temp(⁰ C) | Flow rate(lt/min) | Inlet temp(⁰ C) | Outlet temp (⁰ C) |
| 1 | 0 | 0.6 | 30 | 30 | 1.4 | 30 | 30 |
| 2 | 10 | 0.6 | 64 | 55.5 | 1.4 | 31 | 42 |
| 3 | 15 | 0.6 | 65 | 57 | 1.4 | 34 | 44 |
| 4 | 20 | 0.6 | 65 | 57.5 | 1.4 | 36 | 45.5 |
| 5 | 25 | 0.6 | 65.5 | 58 | 1.4 | 38 | 47 |
| 6 | 30 | 0.6 | 65.5 | 58.5 | 1.4 | 38.5 | 48.5 |
| 7 | 35 | 0.6 | 65.5 | 58.5 | 1.4 | 38.5 | 48.5 |

Again, the same procedure was carried out for 600 ml/min and 1200 ml/min for hot and cold-water flow rates respectively. The table below indicates the temperature reading at that flow rate.

After conducting the experiment at various flow rates better effectiveness was obtained at 600 ml/min and 1200 ml/min flow rates of hot water and cold water respectively. Hence, for hot water 600 ml/min, and for cold water 1200 ml/min flow rates were fixed. The same flow rates are used for the overall experiment.

Experimentation and Analysis of the Heat Transfer Behaviour of the Hybrid Nanofluid (AL₂O₃ + ZnO) in a Parallel Flow Heat Exchanger

Table (13): Temperatures at 0.6 lt/min hot water flow rate data

| S. No | Time | Hot water side | | | Water +Ethylene Glycol | | |
|-------|------|--------------------|-----------------------------|------------------------------|------------------------|-----------------------------|-------------------------------|
| | | Flow Rate(ltr/min) | Inlet temp(⁰ C) | Outlet temp(⁰ C) | Flow rate(ltr/min) | Inlet temp(⁰ C) | Outlet temp (⁰ C) |
| 1 | 0 | 0.6 | 27 | 27 | 1.2 | 27 | 27 |
| 2 | 10 | 0.6 | 65 | 51 | 1.2 | 29.5 | 36.5 |
| 3 | 15 | 0.6 | 65 | 52 | 1.2 | 33 | 40 |
| 4 | 20 | 0.6 | 64.5 | 53 | 1.2 | 36 | 42 |
| 5 | 25 | 0.6 | 64 | 53.5 | 1.2 | 37.5 | 43 |
| 6 | 30 | 0.6 | 64 | 54 | 1.2 | 38.5 | 44 |
| 7 | 35 | 0.6 | 64 | 54 | 1.2 | 39 | 44.5 |
| 8 | 40 | 0.6 | 64 | 54 | 1.2 | 39 | 44.5 |

Case 2: [80:20] [Al₂O₃: ZnO]:

The heat exchanger has been thoroughly cleaned with distilled water and the 5-liter tank was also cleaned properly using distilled water before introducing an 80:20 coolant sample in a 5-liter tank. Initially, the coolant was poured into the 5-liter tank carefully. Measures at the outlet of the heat exchanger were taken properly to avoid any wastage of the Nano-coolant sample. The flow rates of hot and cold fluids in parallel conditions were set at 600 ml/min and 1200 ml/min respectively. The heater was put on, initial temperatures were noted down and the first temperature values were taken after 10 minutes followed by every 5 minutes recording. The process continues until a steady state is attained. The tables shown here represent the readings of temperatures at 600 ml/min and 1200 ml/min flow rates.

Table (14): Temperatures at 0.6 lt/min hot water flowrate data with Nanofluid

| S. No | Time | Hot water side | | | Nanofluid | | |
|-------|------|-------------------|-----------------------------|------------------------------|-------------------|-----------------------------|-------------------------------|
| | | Flow Rate(lt/min) | Inlet temp(⁰ C) | Outlet temp(⁰ C) | Flow rate(lt/min) | Inlet temp(⁰ C) | Outlet temp (⁰ C) |
| 1 | 0 | 0.6 | 30 | 30 | 1.2 | 30 | 30 |
| 2 | 10 | 0.6 | 63 | 52.5 | 1.2 | 34.5 | 42 |
| 3 | 15 | 0.6 | 61 | 53 | 1.2 | 36.5 | 43.5 |
| 4 | 20 | 0.6 | 61 | 51 | 1.2 | 38.5 | 45 |
| 5 | 25 | 0.6 | 61 | 49 | 1.2 | 39 | 45.5 |
| 6 | 30 | 0.6 | 60.5 | 49 | 1.2 | 41 | 46 |
| 7 | 35 | 0.6 | 60 | 48 | 1.2 | 42 | 47 |
| 8 | 40 | 0.6 | 60 | 48 | 1.2 | 42 | 47 |

Case 3: [50:50] [Al₂O₃: ZnO]:

A 50:50 sample was poured carefully into the 5 liters tank with all valves closed assuring no coolant loss at the outlet of the heat exchanger. The sample mixture was mixed using a foot pipe to regulate a uniform mixture without any precipitation beneath the tank. Flow rates had been set at 600 ml/min and 1200 ml/min for hot and cold fluids respectively. Parallel valves were opened, and the heater was switched on and the initial temperature values were noted down. The first reading was taken after 10 minutes followed by every 5 minutes recording. The process continues until a steady state is attained. The table below represents the readings of inlet and outlet temperatures of hot & cold fluids.

Table (15): Temperatures at 0.6 lt/min hot water flowrate data with

| S. No | Time | Hot water side | | | Nanofluid | | |
|-------|------|-------------------|----------------|-----------------|-------------------|----------------|------------------|
| | | Flow Rate(lt/min) | Inlet temp(°C) | Outlet temp(°C) | Flow rate(lt/min) | Inlet temp(°C) | Outlet temp (°C) |
| 1 | 0 | 0.6 | 30 | 30 | 1.2 | 30 | 30 |
| 2 | 10 | 0.6 | 62 | 51 | 1.2 | 35 | 41 |
| 3 | 15 | 0.6 | 61.5 | 52 | 1.2 | 36 | 42.5 |
| 4 | 20 | 0.6 | 61.5 | 52.5 | 1.2 | 37 | 43 |
| 5 | 25 | 0.6 | 61.5 | 53 | 1.2 | 38 | 44 |
| 6 | 30 | 0.6 | 61.5 | 53 | 1.2 | 39 | 44 |

Case 4: [60:40] [Al₂O₃: ZnO]:

60:50 sample was poured carefully into the 5 liters tank with all valves closed assuring no coolant loss at the outlet of the heat exchanger. The sample mixture was mixed using a foot pipe to regulate a uniform mixture without any precipitation beneath the tank. Flow rates had been set at 600 ml/min and 1200 ml/min for hot and cold fluids respectively. Parallel valves were opened, and the heater was switched on and the initial temperature values were noted down. The first reading was taken after 10 minutes followed by every 5 minutes recording. The process continues until a steady state is attained. The table below represents the readings of inlet and outlet temperatures of hot & cold fluids.

Table (16): Temperatures at 0.6 lt/min hot water flowrate data with Nanofluid

| S. No | Time | Hot water side | | | Nanofluid | | |
|-------|------|-------------------|-----------------------------|------------------------------|-------------------|-----------------------------|-------------------------------|
| | | Flow Rate(lt/min) | Inlet temp(⁰ C) | Outlet temp(⁰ C) | Flow rate(lt/min) | Inlet temp(⁰ C) | Outlet temp (⁰ C) |
| 1 | 0 | 0.6 | 30 | 30 | 1.2 | 30 | 30 |
| 2 | 10 | 0.6 | 62 | 49 | 1.2 | 30 | 37 |
| 3 | 15 | 0.6 | 63.5 | 50.5 | 1.2 | 33 | 39.5 |
| 4 | 20 | 0.6 | 63.5 | 51.5 | 1.2 | 36 | 41 |
| 5 | 25 | 0.6 | 63.5 | 51 | 1.2 | 38 | 42 |
| 6 | 30 | 0.6 | 63.5 | 51 | 1.2 | 38 | 42 |

Since this was the last coolant sample, the heat exchanger had to be cleaned thoroughly using cleaning acid. Acid wash was deployed to clean the insides of the tubes and very little precipitate of nano-powder was found. After a series of flushing processes, the heat exchanger was finally run on water with varying flow rates on cold side satisfying no harm is done to the equipment.

The table below represents the final temperature values of all samples

Experimentation final values:

Table (17): Final Temperatures at 0.6 lt/min hot water flowrate data with different samples

| S. No | Sample Name | Hot water flow rate | (T _{hi}) | (T _{ho}) | Cold water flow rate | (T _{ci}) | (T _{co}) |
|-------|-------------|---------------------|--------------------|--------------------|----------------------|--------------------|--------------------|
| 1 | DW +MEG | 600 | 64 | 54 | 1200 | 39 | 44.5 |
| 2 | 80:20 | 600 | 60 | 48 | 1200 | 42 | 47 |
| 3 | 60:40 | 600 | 63.5 | 51 | 1200 | 38 | 42 |
| 4 | 50:50 | 600 | 61.5 | 53 | 1200 | 39 | 44 |

6. CFD ANALYSIS:

Building the required geometry and mesh for modeling the dominion is the first step in the analysis of the system known as computational fluid dynamics, or CFD. The process of discretizing the domain into tiny volumes and using iterative techniques to solve the equations is known as meshing. Beginning with the description of the dominion's boundaries and initial

conditions, modeling progresses to modeling the complete system. Analyzing the findings, drawing conclusions, and having debates come next.

Geometry: -

The ANSYS workbench design module includes heat exchangers. This heat exchanger is counter-flow. First, the workbench's fluid flow (fluent) module is chosen. Double-clicking the geometry opens the design model in a new window.

Sketching: Out of the three planes viz., XY-plane, YZ-plane and ZX-plane, the XY-plane is selected for the first sketch. A circle of diameter 33.5mm & another circle with diameter 27.5mm is drawn by selecting the circle in sketching tab menu. Similarly, by selecting again XY-plane and draw another sketch with two circles having diameter 14mm and 8.5mm.

Extrude: By selecting the first sketch in XY-plane extrude it up to 2mm length as an outer pipe. Again, select another sketch Extrude up 2m & name as inner pipe and change its operation from material to add frozen in Z-direction and change operation and material to add frozen. By extruding the whole body and by changing operation from adding material to adding frozen we have four different parts and four bodies.

Mesh: Meshing for both cases of Double pipe heat exchanger is done in ANSYS meshing where different methods of meshing are used for different zones of Double pipe heat exchanger model. There are basically two zones, one is solid, and the second one is fluid. So, in this project, two fluid zones i.e. crude oil and diesel oil are used and inner pipe, outer pipe and fins come in solid zone based on that whole model is divided into three zone i.e. Inner pipe fluid zone, outer pipe fluid zone and solid zone of inner pipe and outer pipe and fins

Named Selection: According to the necessary inlets and outlets for inner and exterior fluids, the solid's various surfaces are given names. An insulating surface is the name given to the outer wall. At this stage, exit the window and save the project once more. Update and refresh the workbench project. The setup is now available. A window with the ANSYS Fluent Launcher will open. Click OK after selecting 3D dimensions, Double Precision, and Serial Processing. The window for Fluent will open.

Solution: -

Models: Energy is set to ON positions. Viscous model is selected as “k-ε model”.

Materials: The create/edit option is clicked to add water-liquid and steel to the list of fluid and solid respectively from the fluent database.

Cell zone conditions: Inner and outer fluid assigned as water and inner and outer solid pipe assigned as material steel.

Boundary Conditions: Boundary conditions are applied based on the model's requirements. Mass flow inlet and pressure outlet are the definitions of the inlet and outflow circumstances. Given that there are two inlets and two outputs, this is a counter-flow and parallel flow with two tubes. Each wall has its own specification along with the corresponding boundary requirements. For every wall, no slip circumstances are considered. Every wall is set to zero heat flow condition, except for the tube walls.

Solution Control and Initialization:

Under relaxation Factors the parameters are:

- Pressure=0.3 Pascal
- Density=1 kg/m³
- Body forces=1 kg/m² s²
- Momentum=0.7kg-m/s.
- Turbulent kinetic energy=0.8m² /s².

Measure of Convergence:

It is tried to have a nice convergence throughout the simulation and hence criteria are made strict to get an accurate result. For this reason, residuals are given as per the table that follows

Table (18): Convergence Residuals

| Variable | Residual |
|--|------------------|
| X-Velocity | 10 ⁻⁶ |
| Y-Velocity | 10 ⁻⁶ |
| Z-Velocity | 10 ⁻⁶ |
| Continuity | 10 ⁻⁵ |
| Specific dissipation energy/Dissipation energy | 10 ⁻⁵ |
| Turbulent Kinetic Energy | 10 ⁻⁵ |
| Energy | 10 ⁻⁹ |

Run Calculation:

The number of iterations is set to 400 and the solution is calculated, and various contours, vectors, and place are obtained.

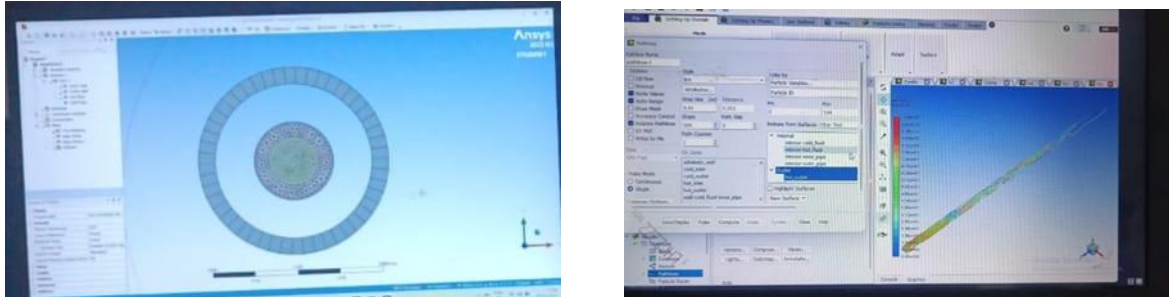


Fig (9): Simulation results

Simulation and experimentation comparison table

Table (19): Comparison table between experimental and simulation values

| S. No | Sample Name | Experimentation | | | | Simulation | | | |
|-------|-------------|-----------------|-----------------|-----------------|-----------------|-----------------|-----------------|-----------------|-----------------|
| | | T _{hi} | T _{ho} | T _{ci} | T _{co} | T _{hi} | T _{ho} | T _{ci} | T _{co} |
| 1 | DW+MEG | 64 | 54 | 39 | 44.5 | 64 | 54.13 | 39 | 46.19 |
| 2 | 80:20 | 60 | 48 | 42 | 47 | 60 | 47.34 | 42 | 46 |
| 3 | 60:40 | 63.5 | 51 | 38 | 42 | 63.5 | 49.32 | 38 | 45.34 |
| 4 | 50:50 | 61.5 | 53 | 39 | 44 | 61.5 | 54.26 | 39 | 45 |

7. PERFORMANCE PARAMETERS

All the properties that are vital to determine the heat transfer performance of the coolant samples are obtained (density, specific heat) along with their readings on heat exchanger. Therefore, the foremost calculation that had to be carried out was heat transfer(Q) from the hot fluid and cold fluid. Followed by logarithmic mean temperature difference (LMTD), overall heat transfer coefficient (OHTC), and effectiveness (ϵ).

Heat transfer (Q):

Heat transfer from hot fluid $Q_w = m_w C_w (T_{hi} - T_{ho})$

Heat transfer from the coolant $Q_c = m_c C_c (T_{co} - T_{ci})$

Mass flow rate can be achieved in kg/sec from the following relation

Experimentation and Analysis of the Heat Transfer Behaviour of the Hybrid Nanofluid (AL₂O₃ + ZnO) in a Parallel Flow Heat Exchanger

$$m \text{ kgsec} = \text{density} \times \text{volume} \times 60$$

Calculating appropriate values of heat capacity, temperature difference for parallel flow condition and for variable flow rates following results are obtained corresponds to the heat transfer rate in watts for all coolant samples.

Table (20): Heat transfer results for all coolant samples (experimental & simulation)

| S. No | Sample name | Experimental | | | Simulation | | |
|-------|-------------|--------------|-------------|---------|------------|-------------|---------|
| | | Q(hotside) | Q(coldside) | Q Avg | Q(hotside) | Q(coldside) | Q Avg |
| 1 | DW +MEG | 418.6 | 381.48 | 400.04 | 413.15 | 499.25 | 456.205 |
| 2 | 60:40:00 | 523.25 | 276.744 | 399.27 | 593.57 | 507.82 | 550.7 |
| 3 | 50:50:00 | 355.81 | 345.52 | 350.665 | 302.92 | 414.68 | 358.77 |
| 4 | 80:20:00 | 502.32 | 343.698 | 424.009 | 529.11 | 276.58 | 402.83 |

Logarithmic Mean Temperature Difference (LMTD):

LMTD can be determined by the final four temperatures (T_{hi}, T_{ho}, T_{ci}, T_{co}) obtained at steady state condition. A typical parallel flow heat transfer illustrates in the form of a graph is given as:

Equations below give the LMTD for the parallel flow heat exchanger.

$$\text{Parallel flow: } (T_{hi} - T_{ci}) - (T_{ho} - T_{co}) \ln \left[\frac{(T_{hi} - T_{co})}{(T_{ho} - T_{ci})} \right] (\Delta T_1 \Delta T_2)$$

Where T_{hi} – Inlet temperature of the hot fluid

T_{ho} – Outlet temperature of the hot fluid

T_{ci} – Inlet temperature of the cold fluid

T_{co} – Outlet temperature of the cold fluid

ΔT₁ - Temperature difference at the left side

ΔT₂ – Temperature difference at the right side

Upon substituting the values in the above equation, we get parallel flow Logarithmic Mean Temperature Difference both in Experimental and Simulation.

Table (21): LMTD

| S. No | Sample Name | Overall Heat Transfer Coefficient | |
|-------|-------------|-----------------------------------|-----------------|
| | | Simulation | Experimentation |
| 1 | DW+MEG | 177.56 | 144.61 |
| 2 | 60:40 | 275.24 | 144.14 |
| 3 | 50:50 | 138.98 | 137.78 |
| 4 | 80:20 | 363.5524 | 417.35 |

Overall Heat Transfer Coefficient (OHTC):

OHTC can be stated as the amount of heat required to raise the temperature of the substance by a single degree for a square meter area. It can be determined by using the relation:

$$U = QA.LMTD$$

Where, Q = Heat transfer from the fluid in W or J/s

A = Area of the heat exchanger in m²

U = OHTC in W/m²°C

Values pertaining to OHTC can be substituted and evaluated for both experimental and simulation values.

Table (22): OHTC Results

| S. No | Sample Name | Logarithmic Mean Temperature Difference | |
|-------|-------------|---|----------------------|
| | | Simulation (°C) | Experimentation (°C) |
| 1 | DW+ MEG | 14.87 | 16.01 |
| 2 | 60:40:00 | 11.58 | 15.84 |
| 3 | 50:50:00 | 14.91 | 14.73 |
| 4 | 80:20:00 | 6.413 | 5.88 |

Effectiveness (ϵ):

Effectiveness of a heat exchanger is evaluated as the ratio of actual heat transfer to the maximum heat transfer among the fluids. Therefore, value of Effectiveness is always less than

Experimentation and Analysis of the Heat Transfer Behaviour of the Hybrid Nanofluid (AL₂O₃ + ZnO) in a Parallel Flow Heat Exchanger

1 and is represented in the form of percentage. In general, actual heat transfer refers to heat transfer from the hot fluid and the maximum heat transfer is taken as the minimum heat capacity between the hot and cold fluid and the maximum temperature difference, which is usually hot inlet and cold inlet temperature.

$$\varepsilon = \frac{Q}{Q_{\max}}$$

Effectiveness of parallel flow heat exchanger for both experimentation and simulation values are shown below:

Table (23): Effectiveness results

| S. No | Sample Name | Effectiveness (%) | |
|-------|-------------|-------------------|-----------------|
| | | Simulation | Experimentation |
| 1 | DW+MEG | 39.44 | 40 |
| 2 | 60:40:00 | 55.6 | 49.01 |
| 3 | 50:50:00 | 32.28 | 37.7 |
| 4 | 80:20:00 | 72.2 | 66.6 |

8. RESULTS

RESULTS: Pertaining to all the values obtained in calculations unit, this section demonstrates the results, comparison between all the coolant samples and the conclusions. During the time of experimentation, sample 80:20 was found practically most effective upon reviewing the readings that were simultaneously obtained. Conclusively, maximum proportion of Aluminium Oxide exhibited maximum heat transfer performance because of its ability to absorb and release the heat.

Logarithmic Mean Temperature Difference (°C):

LMTD in °C for all the coolant samples for parallel flow conditions when the flow rate is 600 ml/min and 1200 ml/min for hot fluid & cold fluid respectively. The following graph shows the comparison of LMTD values between experimentation and simulation.

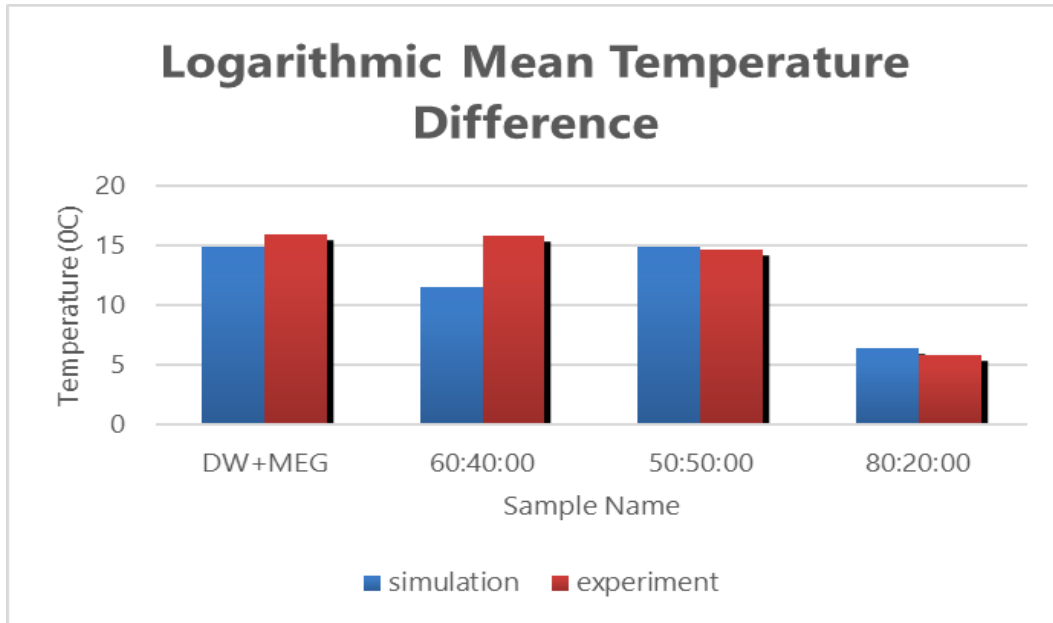


Fig (10): LMTD at parallel flow for both simulation and experimentation

Effectiveness (ϵ) :

Effectiveness of all samples at parallel flow conditions for 600 ml/min and 1200 ml/min for hot & cold fluid respectively. The following graph shows the comparison of Effectiveness values between experimentation and simulation.

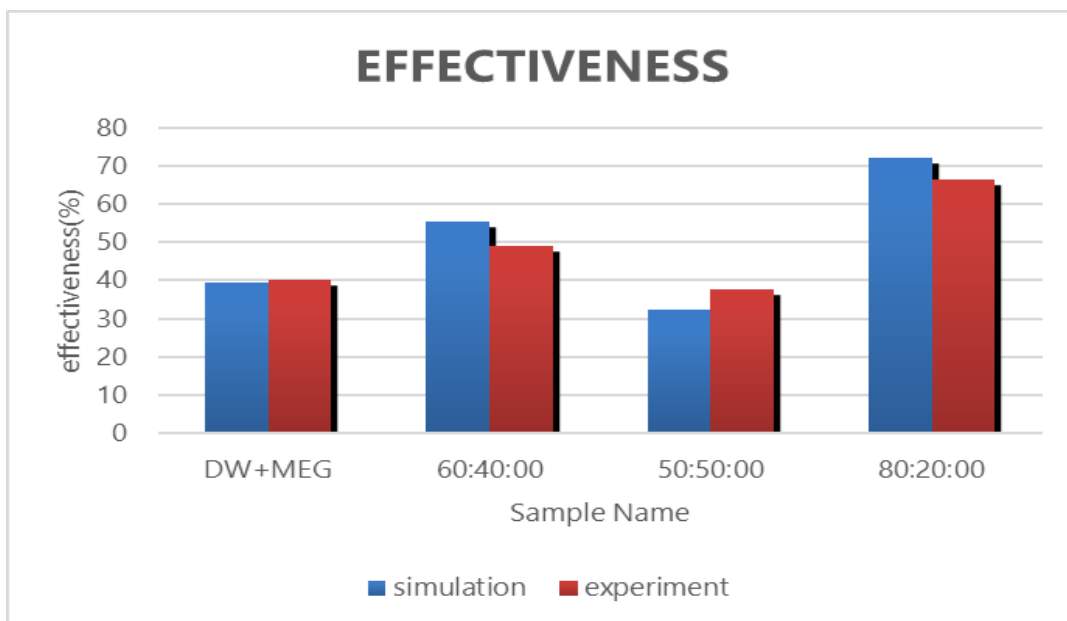


Fig (11): Effectiveness values both simulation and experimentation

Overall Heat Transfer Coefficient (OHTC):

The OHTC of all samples at parallel flow conditions for 600 ml/min and 1200 ml/min for hot & cold fluid respectively. The following graph shows the comparison of OHTC values between experimentation and simulation.

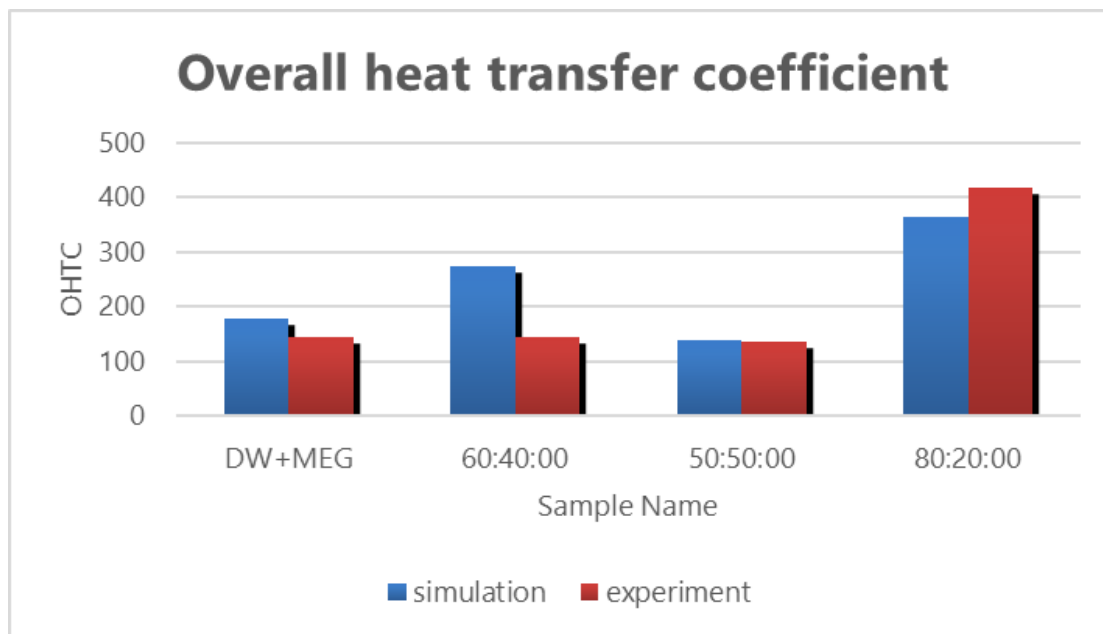


Fig (12): OHTC values for simulation and experimentation

Heat Transfer Rate (Watts):

The Heat Transfer Rate of all samples at parallel flow conditions for 600 ml/min and 1200 ml/min for hot & cold fluid respectively. The following graph shows the comparison of Average Heat Transfer Rate values between experimentation and simulation.

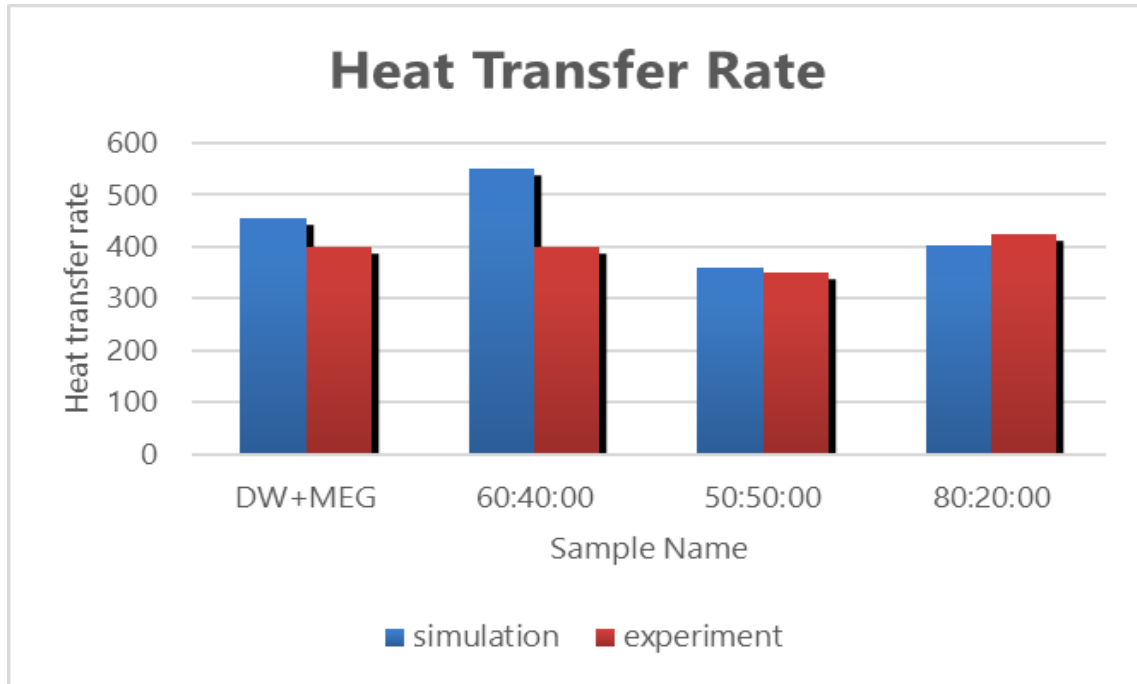


Fig (13): Average Heat Transfer Rate values for both simulation and experimentation

9. CONCLUSIONS

Using Al_2O_3 and ZnO hybrid nanoparticles in 50:50, 60:40, and 80:20 mixture ratios with a 0.1% volume concentration in DW+MEG (60:40) on a double pipe shell & tube heat exchanger with various flow rates, this study was conducted on nano coolants. Nano coolant samples HTR, LMTD, OHTC, and Effectiveness were subjected to parallel flow calculations and analysis. The thermo-physical properties of the combination are greatly enhanced when metal oxide hybrid nanoparticles are suspended in the base fluid. The following are the results of a thermal experimental examination of nano fluids on heat exchangers, their impact in comparison to traditional coolants, and their prospective heat transfer applications, particularly nano coolants in radiators:

Among all the samples, the coolant sample 80:20 (Al_2O_3 : ZnO) had the highest rate of efficiency, increasing by 35% when compared to both water and the conventional sample DW+MEG. An additional 50–100 watts of heat transmission have been noted in the case of parallel flow, and the average heat transfer rate rises as the percentage ratio of Al_2O_3 increases. When the flow rate was set at 0.6L/min, its overall heat transfer coefficient was noticeably higher than that of other compositions. All coolant samples had a comparable logarithmic mean

temperature difference (LMTD); nevertheless, there was a minor variation in each sample, with sample 60:40 having the greatest LMTD. Due to the continuous circulation of coolant samples into the heat exchanger system. A small degree of aggregation was seen, demonstrating the hybrid nanoparticles' strong stability in the base fluid. Due to faults in the traditional heat exchanger, all coolant samples were determined to be more effective during the simulation period than the experimentation values; nonetheless, the pattern of increase or reduction is comparable in both circumstances. When the readings were taken simultaneously during the experiment, sample 80:20 was determined to be practically the most effective. Compared to the base fluid (DW+MEG), we can see that the OHTC in 80:20 sample is more than three times greater.

10. FUTURE SCOPE

Analysis of exact mixture ratios and their stability in the process requires much more attention because the heat transfer performance is determined by the ideal volume fraction of nanoparticles suspended in the base fluid. Among the main things to address in the future are anti-corrosion qualities, lowering agglomerations, clogging, and their impact on interacting material. To learn more about the performance of heat transmission, different types of tribrid and poly nanoparticles at different volume proportions can be studied. The chemical characteristics of the hybrid nanoparticles that will be distributed in the base fluid must be thoroughly investigated; this will undoubtedly enhance the thermo-physical qualities. To cool the gasket and prevent heat emissions from the engine, a new, small model that may be used as an air conditioner near the engine cylinder head has been developed. examining how hybrid nanofluids affect the pumping power and pressure drop needed in double pipe heat exchangers. To increase the stability and homogeneity of the hybrid nanofluids, new techniques for creating and dispersing the nanoparticles in the base fluid must be developed. Assessing the hybrid nanofluids' long-term stability, dependability, and durability in double pipe heat exchangers by numerical simulations and experimental investigations.

11. REFERENCES

- [1] Avdhoot Jejurkar, Piyush Singh, Atik Shaikh, Sahu Kirankanta, 2Sharif Mozzamil, Heat transfer enhancement using various nano fluids –A REVIEW, International Research Journal of Engineering and Technology (IRJET), **Volume: 05 Issue: 11 | Nov 2018.**
- [2] Kim, P., Shi, L., Majumdar, A., and McEuen, P. L., Thermal Transport Measurements of Individual Multiwalled Nanotubes, *Physical Review Letters*, vol. 87, no. 21, pp. 215502–1–4, 2001.
- [3] Wen, D., Lin, G., Vafaei, S., & Zhang, K. (2009). Review of nanofluids for heat transfer applications. *Particuology*, 7(2), 141–150. doi:10.1016/j.partic.2009.01.007.
- [4] Bowers, J., Cao, H., Qiao, G., Li, Q., Zhang, G., Mura, E., & Ding, Y. (2018). Flow and heat transfer behaviour of nanofluids in microchannels. *Progress in Natural Science: Materials International*, 28(2), 225–234. doi:10.1016/j.pnsc.2018.03.005
- [5] Lee, J., & Mudawar, I. (2007). Assessment of the effectiveness of nanofluids for single-phase and two-phase heat transfer in micro-channels. *International Journal of Heat and Mass Transfer*, 50(3-4), 452–463. doi:10.1016/j.ijheatmasstransfer.
- [6] Wen, D., & Ding, Y. (2004). Experimental investigation into convective heat transfer of nanofluids at the entrance region under laminar flow conditions. *International Journal of Heat and Mass Transfer*, 47(24), 5181–5188. doi:10.1016/j.ijheatmasstransfer.
- [7] R. Y. Chein, J. Chuang, Thermal analysis of nanofluids in microfluidics using an infrared camera, *Int. J. Therm. Sci.* 46 (1) (2007) 57–66.
- [8] Maghrebi, M. J., Nazari, M., & Armaghani, T. (2012). Forced Convection Heat Transfer of Nanofluids in a Porous Channel. *Transport in Porous Media*, 93(3), 401–413. doi:10.1007/s11242-012-9959-2 .
- [9] Nield, D. A., & Kuznetsov, A. V. (2014). Forced convection in a parallel-plate channel occupied by a nanofluid or a porous medium saturated by a nanofluid. *International Journal of Heat and Mass Transfer*, 70, 430–433. doi:10.1016/j.ijheatmasstransfer .
- [10] Koo, J., & Kleinstreuer, C. (2005). Impact analysis of nanoparticle motion mechanisms on the thermal conductivity of nanofluids. *International Communications in Heat and Mass Transfer*, 32(9), 1111–1118. doi:10.1016/j.icheatmasstransfer.

- [11] Ragui, K., Bennacer, R., & El Ganaoui, M. (2021). Oscillatory flow of Koo–Kleinstreuer and aggregate nanofluids in cylindrical annuli: Toward an innovative solution to deal with nanofluids instability. *Physics of Fluids*, 33(4), 042013. doi:10.1063/5.0046784.
- [12] Xuan, Y., & Li, Q. (2000). Heat transfer enhancement of nanofluids. *International Journal of Heat and Fluid Flow*, 21(1), 58–64. doi:10.1016/s0142-727x(99)00067-.
- [13] Kumar, P., & Sarviya, R. M. (2021). Recent developments in preparation of nanofluid for heat transfer enhancement in heat exchangers: A review. *Materials Today: Proceedings*, 44, 2356–2361. doi:10.1016/j.matpr.2020.12.434.
- [14] O.O. Oyeleke, O.S. Ohunakin, D.S. Adelekan, O.E. Atiba, M.O. Nkiko and G. Jatinder, Recent Advancements in the Development of Nanofluid Technology in Heat Transfer Applications, <https://iopscience.iop.org/volume/1757-899X/1107>.
- [15] Zohuri, B. (2016). Heat Exchanger Types and Classifications. *Compact Heat Exchangers*, 19–56. doi:10.1007/978-3-319-29835-1_2
- [16] [16]. Louis, S.P.; Ushak, S.; Milian, Y.; Nem's, M.; Nem's, A. Application of Nanofluids in Improving the Performance of Double-Pipe Heat Exchangers—A Critical Review. *Materials* **2022**, 15,6879. <https://doi.org/10.3390/ma15196879>.
- [17] Simpson, S., Schelfhout, A., Golden, C., & Vafaei, S. (2018). Nanofluid Thermal Conductivity and Effective Parameters. *Applied Sciences*, 9(1), 87. doi:10.3390/app9010087
- [18] Li, C.H.; Peterson, G.P. Experimental investigation of temperature and volume fraction variations on the effective thermal conductivity of nanoparticle suspensions (nanofluids). *J. Appl. Phys.* 2006, 99, 084314.
- [19] Hussein, A. M., Bakar, R. A., & Kadrigama, K. (2014). Study of forced convection nanofluid heat transfer in the automotive cooling system. *Case Studies in Thermal Engineering*, 2, 50–61. doi:10.1016/j.csite.2013.12.001
- [20] Pang, C.; Jung, J.Y.; Lee, J.; Kang, Y. Thermal conductivity measurement of methanol-based nanofluids with Al_2O_3 and SiO_2 nanoparticles. *Int. J. Heat Mass Transf.* 2012, 55, 5597–5602.
- [21] Yoo, D.; Hong, K.S.; Yang, H.S. Study of thermal conductivity of nanofluids for the application of heat transfer fluids. *Thermochim. Acta* 2007, 455, 66–69.

- [22] Gupta, M.; Singh, V.; Kumar, R.; Said, Z. A review on thermophysical properties of nanofluids and heat transfer applications. *Renew. Sustain. Energy Rev.* **2017**, *74*, 638–670.
- [23] Ciornei, F.C.; Alaci, S.; Amarandei, D.; Irimescu, L.; Romanu, I.C.; Acsinte, L.I. Method and Device for Measurement of Dynamic Viscosity. In *IOP Conference Series: Materials Science and Engineering*, Proceedings of the 13th International Conference on Tribology, ROTRIB'16, Galati, Romania, 22–24 September 2016; IOP Publishing: Bristol, UK, 2017; Volume 174, p. 2017012041.
- [24] Zahmatkesh, I.; Sheremet, M.; Yang, L.; Heris, S.Z.; Sharifpur, M.; Meyer, J.P.; Ghalambaz, M.; Wongwises, S.; Jing, D.; Mahian, O. Effect of nanoparticle shape on the performance of thermal systems utilizing nanofluids: A critical review. *J. Mol. Liq.* **2021**, *321*, 114430.
- [25] Dalkılıç, A.S.; Mercan, H.; Özçelik, G.; Wongwises, S. Optimization of the finned double-pipe heat exchanger using nanofluids as working fluids. *J. Therm. Anal.* **2021**, *143*, 859–878.
- [26] Asokan, N.; Gunnasegaran, P.; Wanatasanappan, V.V. Experimental investigation on the thermal performance of compact heat exchanger and the rheological properties of low concentration mono and hybrid nanofluids containing Al₂O₃ and CuO nanoparticles. *Therm. Sci. Eng. Prog.* **2020**, *20*, 100727.
- [27] Osman, S.; Sharifpur, M.; Meyer, J.P. Experimental investigation of convection heat transfer in the transition flow regime of aluminium oxide-water nanofluids in a rectangular channel. *Int. J. Heat Mass Transf.* **2019**, *133*, 895–902.
- [28] Kavitha, R.; Algani, Y.M.A.; Kulkarni, K.; Gupta, M. Heat transfer enhancement in a double pipe heat exchanger with copper oxide nanofluid: An experimental study. *Mater. Today Proc.* **2021**, *56*, 3446–3449.
- [29] Bahmani, M.H.; Sheikhzadeh, G.; Zarringhalam, M.; Akbari, O.A.; Alrashed, A.A.; Shabani, G.A.S.; Goodarzi, M. Investigation of turbulent heat transfer and nanofluid flow in a double pipe heat exchanger. *Adv. Powder Technol.* **2018**, *29*, 273–282.
- [30] Bahmani, M.H.; Akbari, O.A.; Zarringhalam, M.; Shabani, G.A.S.; Goodarzi, M. Forced convection in a double tube heat exchanger using nanofluids with constant and variable thermophysical properties. *Int. J. Numer. Methods Heat Fluid Flow* **2019**, *30*, 3247–3265.
- [31] Poongavanam, G.K.; Panchabikesan, K.; Murugesan, R.; Duraisamy, S.; Ramalingam, V. Experimental investigation on heat transfer and pressure drop of MWCNT-Solar glycol based nanofluids in shot peened double pipe heat exchanger. *Powder Technol.* **2019**, *345*, 815–824.

Experimentation and Analysis of the Heat Transfer Behaviour of the Hybrid Nanofluid ($\text{Al}_2\text{O}_3 + \text{ZnO}$) in a Parallel Flow Heat Exchanger

- [32] Zheng, D.; Wang, J.; Pang, Y.; Chen, Z.; Sunden, B. Heat transfer performance and friction factor of various nanofluids in a double-tube counter flow heat exchanger. *Therm. Sci.* **2020**, *24*, 3601–3612.
- [33] Zheng, D.; Wang, J.; Chen, Z.; Baleta, J.; Sundén, B. Performance analysis of a plate heat exchanger using various nanofluids. *Int. J. Heat Mass Transf.* **2020**, *158*, 119993.
- [34] J. Routbort et al., Argonne National Lab, Michellin North America, St. Gobain Corp., 2009, <http://www1.eere.energy.gov/industry/nanomanufacturing/pdfs/nanofluidsindustrialcooling.pdf>.
- [35] Wong KV, De Leon O. Applications of Nanofluids: Current and Future. *Advances in Mechanical Engineering.* 2010;2. doi:10.1155/2010/519659
- [36] E. M. Hamad, B. Sawalmeh, A. A. Mhawsh, M. Mansour, M. Awad, A. T. Al-Halhouli, and S. I. Al-Gharabli, 2019 41st Annual International Conference of the IEEE Engineering in Medicine and Biology Society (EMBC) (2019), Vol. 2013, Article ID: 825376
- [37] F. Liang, Y. Qiao, M. Duan, N. Lu, J. Tu, and Z. Lu, A high pressure nanofluidic micro-pump based on H_2O electrolysis. 2018, IEEE International Conference on Manipulation, Manufacturing and Measurement on the Nanoscale (3M-NANO), edited by M. Yu, and Z. Weng, Institute of Electrical and Electronics Engineers Inc., pp. 32–36 (2018).
- [38] Kao M. J., Lo C. H., Tsung T. T., Wu Y. Y., Jwo C. S., and Lin H. M., “Copper-oxide brake nanofluid manufactured using arc-submerged nanoparticle synthesis system,” *Journal of Alloys and Compounds*, vol. 434-435, pp. 672–674, 2007.
- [39] Kao M. J., Lo C. H., Tsung T. T., Wu Y. Y., Jwo C. S., and Lin H. M., “Copper-oxide brake nanofluid manufactured using arc-submerged nanoparticle synthesis system,” *Journal of Alloys and Compounds*, vol. 434-435, pp. 672–674, 2007.
- [40] Wole-Osho, I., Okonkwo, E. C., Kavaz, D., & Abbasoglu, S. (2020). An experimental investigation into the effect of particle mixture ratio on specific heat capacity and dynamic viscosity of $\text{Al}_2\text{O}_3\text{-ZnO}$ hybrid nano fluids. *Powder Technology*. doi:10.1016/j.powtec.2020.01.015
- [41] Sidik, N. A. C., Adamu, I. M., Jamil, M. M., Kefayati, G. H. R., Mamat, R., & Najafi, G. (2016). Recent progress on hybrid nanofluids in heat transfer applications: A comprehensive review. *International Communications in Heat and Mass Transfer*, *78*, 68-79. doi:10.1016/j.ic

heat mass transfer. Naseema, NawazishMehdia, S., Manzoor Hussain, M., Khader Basha, S., & Abdul Samad, M. (2018). Heat Enhancement Of Heat Exchanger Using Aluminium Oxide(Al_2O_3), Copper Oxide(CuO)Nano Fluids With Different Concentrations. Materials Today: Proceedings, 5(2), 6481–6488. doi:10.1016/j.matpr.2017.12.261.

Citation: Veerababu Divili. Experimentation and Analysis of the Heat Transfer Behaviour of the Hybrid Nanofluid ($Al_2O_3 + ZNO$) in a Parallel Flow Heat Exchanger. International Journal of Thermal Engineering (IJTE), 13(1), 2025, pp. 1-38.

Abstract Link: https://iaeme.com/Home/article_id/IJTE_13_01_001

Article Link:

https://iaeme.com/MasterAdmin/Journal_uploads/IJTE/VOLUME_13_ISSUE_1/IJTE_13_01_001.pdf

Copyright: © 2025 Authors. This is an open-access article distributed under the terms of the Creative Commons Attribution License, which permits unrestricted use, distribution, and reproduction in any medium, provided the original author and source are credited.

Creative Commons license: Creative Commons license: CC BY 4.0



✉ editor@iaeme.com